

Stabilizing Chromium from Leather Waste in Biochar

Hannah C. Wells,[†] Katie H. Sizeland,[†] Richard L. Edmonds,[‡] William Aitkenhead,[‡] Peter Kappen,[§] Chris Glover,[§] Bernt Johannessen,[§] and Richard G. Haverkamp^{*,†}

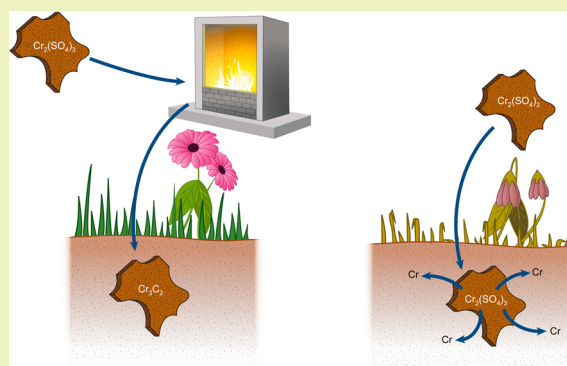
[†]School of Engineering and Advanced Technology, Massey University, Private Bag 11222, Palmerston North 4442, New Zealand

[‡]Leather and Shoe Research Association, P.O. Box 8094, Palmerston North 4446, New Zealand

[§]Australian Synchrotron, 800 Blackburn Road, Clayton, Victoria 3168, Australia

ABSTRACT: Disposal of chrome-tanned leather waste provides an environmental challenge, with land-based methods risking leaching of chromium into the environment. We investigate the production of biochar from leather as an alternative means to dispose of leather waste. Chrome-tanned leather is heated at 500–1000 °C in an environment excluding oxygen to form biochar. The char is leached in 1 M HCl for 15 h, and the leachate is analyzed for Cr to confirm that Cr does not leach from char formed at or above 600 °C. The char is analyzed by X-ray absorption spectroscopy (XAS) for chemical state and structure. X-ray absorption near edge structure (XANES) analysis shows that the leather and biochar contain Cr as a mixture of Cr sulfate and Cr carbide, with the proportion of Cr as carbide increasing from 0% for untreated leather to 88% for char formed at 1000 °C. Modeling of the extended X-ray absorption fine structure (EXAFS) spectra shows that the atomic near-range structure is consistent with that of chromium carbide for the high-temperature samples. Biochar produced from chrome-tanned leather waste contains highly dispersed chromium present as a stable, carbide-like structure (provided sufficiently high temperatures are used). This material, rather than being an environmental problem, may be used for soil remediation and carbon sequestration.

KEYWORDS: Chromium, Biochar, Leather, XAS, Contaminant, Environment



INTRODUCTION

Most leather is produced from skins and hides by tanning with chromium salts, normally $\text{Cr}_2(\text{SO}_4)_3 \cdot x\text{H}_2\text{O}$. Leather is used in upholstery (car and home), shoes, and clothing, but at the end of the life of these goods, the leather needs to be disposed of in an environmentally benign manner. Leather manufacture and production of goods from leather also produce leather scrap which requires disposal. Annual global leather production is about 6.8 million tonnes,¹ around 80% of which is chrome-tanned.

The main concern in the disposal of leather to landfills is the leaching from leather of Cr. Soluble Cr in a hexavalent oxidation state is considered to be undesirable in the environment,^{2,3} and sites where Cr(VI) is present can require remediation.⁴

Current and proposed leather disposal methods include: extraction of Cr before disposal;^{5–7} disposal to wetlands for vegetation to absorb the Cr;⁸ production of other reconstituted structural materials to bind the Cr in new products;^{9,10} and heating leather in an oxidizing environment to create a residue with soluble Cr.^{11,12} Cr contained in or on particulates from the burning of coal and biomass (in the presence of oxygen) can produce Cr(VI).¹³ Therefore, it is possible that burning leather may also generate Cr(VI), which is undesirable.

It has been proposed that the production of biochar, carbonized organic matter, from waste leather may be a better alternative to other disposal methods.¹⁴ Biochar is produced by heating organic matter in an oxygen deficient environment. The application of leather biochar is a method of sequestering carbon, thereby reducing the amount of carbon that may have otherwise become atmospheric CO_2 . Biochar also has the demonstrated benefit of improving agricultural soil productivity.¹⁵ Carbonized leather has previously been considered as a disposal option, with the suggestion of producing an activated carbon product for filtration applications.^{16–18}

Ideally, a leather biochar product could be produced that does not leach Cr. Exposing leather that has been “heat stabilized” in a nonoxidizing environment to leaching indicates that the material has a low solubility of Cr. Specifically, when leather was stabilized at 350 °C or higher in a CO_2 environment, no soluble Cr was detected over a wide pH range in contrast to untreated, chrome-tanned leather.¹⁶ It is also important that the Cr is resistant to oxidation, since both Cr oxidation and reduction between the Cr(III) and Cr(VI) couple¹⁹ can occur in soils, depending on the nature and condition of the soils and

Received: March 24, 2014

Revised: May 12, 2014

Published: June 9, 2014

other factors that control the redox environment. This has led to interest in the analysis of soils for the type of Cr contamination present.^{20,21}

The chemical nature of Cr in leather has been characterized: Cr sulfate is used during tanning, and Cr bonds to the leather's collagen^{22,23} and is well dispersed. However, the form of Cr present in biochar is unknown, as are its stability and dispersion. In an earlier study of the leaching of leather after heat treatment in a nonoxidizing environment, the chemical state of the Cr was not determined.¹⁶

The purpose of the work reported here is to investigate the speciation and structure of the Cr in biochar produced from chrome-tanned leather as a function of the heating conditions. It is intended to confirm the earlier reports of decreased solubility of Cr from leather heated in a nonoxidizing environment and determine that the samples being studied here for Cr speciation do in fact exhibit low Cr solubility. Developing an understanding of the nature of entrapment of Cr in leather biochar may enable a prediction of the likely stability of the Cr in the char in the longer term. For the determination of the chemical speciation and structure of Cr, X-ray absorption spectroscopy (XAS) is used and is known to exhibit obvious spectral differences for different oxidation states and chemical environments.

■ EXPERIMENTAL SECTION

Leather. Standard, commercial chrome-tanned bovine leather was used for all experiments. Raw hides were stripped of hair at 25 °C using 2% w/v sodium hydrosulfide (72% active), 1% w/v sodium sulfide (60% active), 1% hydrated lime, and 0.5% thioglycolic acid (60% active) for 3 h. Next the hides were limed by treating at 28 °C with a solution containing 2% w/v hydrated lime, 1% sodium sulfide (60% active) 0.5% surfactant (nonyl-phenol ethoxylate) for 2 h. Bating followed by treatment with 0.04% (w/w based on hide weight) pancreatic trypsin, followed by tanning with basic Cr sulfate ($\text{Cr}_2(\text{SO}_4)_3 \cdot x\text{H}_2\text{O}$), then retanning with synthetic tannin (Tanicor PW, Clariant), and tara vegetable tannin (Granofin TA, Clariant), followed finally by fatliquoring with a blend of sulfated natural fats.

Pyrolysis Process. The biochar was produced from leather by pyrolysis. The crust leather was stored under ambient conditions prior to pyrolysis. Two pyrolysis reactors were used: a larger unit with no purge gas for the lower-temperature samples (up to 600 °C) and a smaller unit with the sample held under argon for higher-temperature samples (600–1000 °C).

For the larger, lower-temperature reactor, 100 g of leather was placed in a 1 L high-temperature 304 grade stainless-steel reactor. The reactor lid was sealed with a thin layer of potters' clay, and the reactor was flushed with 5 volumes of nitrogen (99.999% pure). The lid contains a nonreturn valve. The reactor was placed in a furnace and heated from ambient to the desired temperature over 1 h, held for 1 h at temperature, and cooled to 100 °C over 3 h before being opened. No control over the atmosphere in the reactor vessel was attempted other than the provision of the nonreturn valve (which resulted in a partial vacuum inside the vessel after cooling).

For the smaller, higher-temperature reactor, 4 g of leather was placed in a 25 mL 304 grade stainless-steel reactor through which a continuous flow of 0.2 L/min argon was passed. The furnace was heated from ambient to the desired temperature and held for 1 h before being rapidly cooled to below 100 °C, at which point the sample was removed; Ar flow was maintained continuously. Three high temperatures were tested, with the following heating and cooling times: heated to 1000 °C over 60 min, held for 60 min, cooled 25 min; heated to 800 °C over 35 min, held for 60 min, cooled 20 min; heated to 600 °C over 50 min, held for 60 min, cooled 5 min. A visual inspection suggested that there was no direct transfer of corrosion product from the stainless steel to the leather char.

Total Chromium Content of Leather and Char. The Cr content of the char and leather samples was measured using a standard industry test method.²⁴ The leather or char is first ashed in air. The residue is then treated with an oxidizing acid (a mixture of 75% v/v perchloric acid (60%, 25% sulfuric acid (98%)) to convert the Cr to hexavalent Cr. The hexavalent Cr is then reduced back to trivalent Cr using iodine in excess and the excess iodine is back-titrated with potassium thiosulfate. All Cr content is represented as weight percent of Cr, regardless of the chemical form.

Leaching of Chromium. Leachable chromium was measured with duplicate samples of char (5 g) leached in 100 mL of 1 M HCl while shaken for 15 h at room temperature. The char material produced was finely ground prior to leaching. The Cr content of the aqueous HCl leachate was then assessed in duplicate with a Varian 220 SpectrAA using a standard industry test method.²⁵

XAS Measurements. X-ray absorption spectra were recorded on the XAS beamline at the Australian Synchrotron, Victoria, Australia. Cr K edge absorption spectra were recorded in transmission mode using a set of flow-through ion chambers supplied with He. The energy was controlled using a fixed exit Si(111) double crystal monochromator. The beam was conditioned using a collimating mirror (Si) and a toroidal focusing mirror (Rh coated). Higher harmonics were rejected using these two mirrors and a flat harmonic rejection mirror (SiO_2). For XAS scans, energy steps of 0.25 eV were employed in the XANES region using 1 s count per step while a step size of 0.035 \AA^{-1} was used in the EXAFS region to 14 \AA^{-1} with count times up of 6 s per step. The energy resolution was about 1 eV, and the photon flux was in the range 10^{11} to 10^{12} photons s^{-1} . The X-ray beam was about $1.5 \times 0.4 \text{ mm}^2$ at the sample. The energy scale was calibrated by simultaneously measuring a Cr foil placed between two downstream ion chambers. Samples were packed in 1 mm thick poly(methyl methacrylate) sample holders. Reference standards were Cr_2O_3 (Prolab), $\text{Cr}_2(\text{SO}_4)_3 \cdot x\text{H}_2\text{O}$ (BDH), $\text{Cr}_2(\text{SO}_4)_3 \cdot x\text{H}_2\text{O}$ (Chromosal B, Lanxess, Germany), $\text{Cr}(\text{CO})_6$ (BDH), Cr_3C_2 (Aldrich), and $\text{Cr}(\text{O}_2\text{C}_5\text{H}_7)_3$ (Aldrich) all diluted with boron nitride (Aldrich). Data processing was performed with ATHENA²⁶ and VIPER.²⁷

■ RESULTS AND DISCUSSION

Biochar Formation. Heating leather under a stream of Ar in the small reactor, or in a larger closed vessel with a pressure release valve, resulted in well-formed char that retained the general shape of the leather feedstock, albeit at a smaller size. Weight loss (from ambient moisture) increased with heating temperature, with 62% weight loss being recorded at 300 °C, 73% at 600 °C, 76% at 800 °C, and 79% at 1000 °C. In the small reactor there was a hint of green color (perhaps Cr_2O_3) on the edge of some char that had formed near the outlet of the reactor suggesting that there was some ingress of oxygen near the outlet. These parts of the sample were not used in the analysis because it is believed they are not representative of the sample and they would not form in a larger scale reactor with better environmental control.

Leachable Cr. It was found that a small amount of Cr can be leached from leather that has not been heat treated (Table 1), as has been reported previously.¹⁶ After heating of the leather, the leachability of Cr diminishes. At 600 °C where the leather is clearly char very little leaching of Cr could be detected (Table 1). In an earlier leaching study it was found that at 350 °C the Cr was no longer able to be leached from the heated leather.¹⁶ It was therefore sought to understand why Cr has much lower solubility from the charred leather.

XANES. X-ray absorption near edge structure (XANES) is a spectroscopic technique that is element specific and is local bonding sensitive. The technique requires irradiating a sample of interest with X-rays across a range of energy that includes an absorption edge. An inspection of the features of the spectrum

Table 1. Initial Chromium Content and Leachable Chromium of Leather and of Biochar Samples Produced under Various Heat Treatments

sample	initial % Cr (SD)	leachable Cr, as % of initial Cr
leather	0.99 (0.01)	4.67
300 °C ^a	2.60 (0.02)	3.50
600 °C ^a	7.39 (0.04)	0.31
600 °C ^b	11.8 (0.8)	0.08
800 °C ^b	12.5 (0.1)	0.06
1000 °C ^b	15.4 (0.1)	0.03

^aLarger reaction vessel. ^bFinely ground, from small reaction vessel.

provides information on the bonding of the element of interest. XANES is most often used in a comparative study between spectra of known standards and unknown samples.

Beam Damage. Alteration to the state of Cr is possible in an intense, focused X-ray beam. The likelihood of this was investigated by doing multiple scans on the same spot of a representative sample and observing differences in the XANES spectra (total collection time up to 2 h). From these measurements it was determined that beam damage is negligible under the conditions that the samples are measured.

XANES of Reference Compounds. In the range of reference compounds for which XAS spectra were collected, it is apparent that there are strong differences in all parts of the spectra including the pre-edge region, the edge energy and the postedge region (Figure 1). It was not possible in this instance

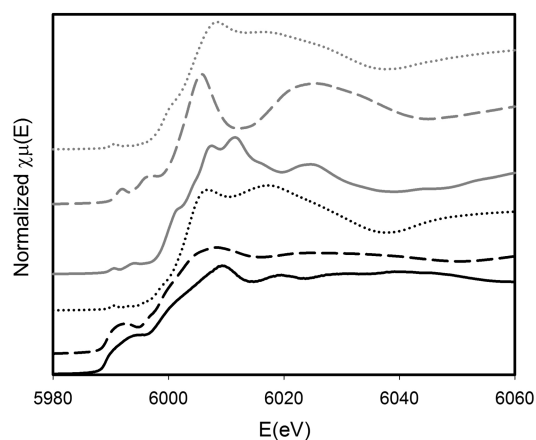


Figure 1. XAS of standards. Cr metal (solid line), Cr₃C₂ (dashed line), Cr(O₂C₃H₇)₃ (dotted line), Cr₂O₃ (grey solid line), CrCO₆ (grey dashed line), Cr₂(SO₄)₃ (grey dotted line).

to analyze any Cr(VI) reference compounds; however, reference spectra are available in the literature^{20,28,29} and always show a strong signature pre-edge feature and a large edge shift.

XANES Edge Position and Cr Oxidation State. The energy position of the absorption edge is very sensitive to the oxidation state of the Cr atom that is excited.^{28,30} The Cr in Cr₃C₂ is seen to have an effective oxidation state similar to that of Cr metal (Figure 1), and the charge on the Cr in Cr₃C₂ is calculated to be +0.33.³¹ One can be confident that there is no Cr(VI) in any of the samples because Cr(VI) has a distinct and sharp pre-edge feature at around 5993.0 eV.^{28,29} The feature arises from nonlocal dipole transitions in Cr(VI) compounds, which are tetrahedrally coordinated.^{32–34} None of the samples showed this pre-edge feature.

XANES of Leather. The XANES spectrum of dried chrome leather is very similar to that of Cr₂(SO₄)₃·xH₂O (Figure 2).

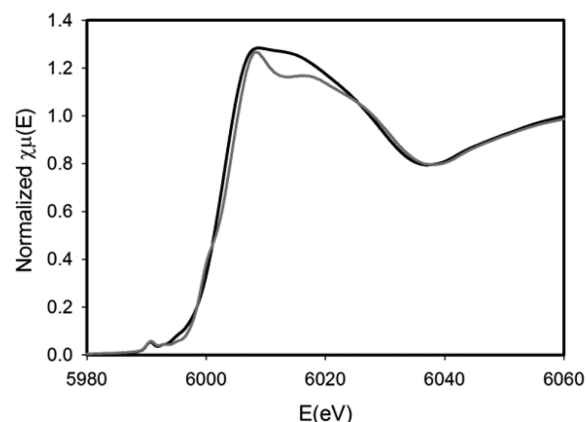


Figure 2. XANES of conditioned chrome tanned leather (solid line) and Cr₂(SO₄)₃·xH₂O (grey solid line).

This is the salt that is used in chrome tanning, so clearly some structural aspects of this salt are retained in the tanned leather. Detailed studies on this subject have been reported previously.^{22,23}

XANES of Biochar. With heating, changes in leather's XANES spectra are observed from 600 °C, with significant differences with each 200 °C increase to the experimental maximum (Figure 3). The spectrum of the sample heated to 600 °C in the larger vessel appears to be equivalent to that of a sample heated to a lower temperature in the small scale vessel. With heating, a pre-edge peak of 5993.4 eV appears and it increases in intensity after higher temperature treatment. The pre-edge peak that forms in the samples at 600 and 800 °C is in the same position as the peak from the Cr₃C₂ standard but is sharper and is not a good match to the shape of the Cr carbide pre-edge peak (or that of any of the standards) and may reflect a different structure to any of the standards. After treatment at 1000 °C, this peak broadens and begins to look more like the Cr carbide pre-edge feature.

A shift in the absorption edge to a lower energy after heating becomes apparent from 800 °C, with a shift of 0.8 eV, and with a further shift apparent at 1000 °C, yielding a total shift of 1.5 eV from the dry leather or chromium sulfate spectrum. The shape of the postedge spectrum changes consistently with heating.

XANES Linear Fits for Biochar. Using the Athena software,²⁶ linear combination fitting to normalized $\chi\mu(E)$ and to $k^3\chi(k)$ were performed. Unconstrained linear combination fitting was attempted using the spectra for Cr₂(SO₄)₃·xH₂O, Cr metal, Cr₂O₃, and Cr₃C₂ (Figure 4). Dry leather is substituted as a proxy for the Cr₂(SO₄)₃·xH₂O spectrum since Cr₂(SO₄)₃·xH₂O is the tanning agent used in chrome-tanned leather and the Cr is well dispersed in leather and therefore gave a better XAS at high k than the ground pure compound mixed with BN. The dry leather better reflects the highly dispersed nature of the Cr. The fit range used was 40 eV below to 70 eV above E₀. Best fits were obtained using only two components, dry leather (or Cr₂(SO₄)₃·xH₂O) and Cr₃C₂ (Figure 5). With an unconstrained fit also containing an initial component of Cr metal or Cr₂O₃, these components do not contribute to the fit. As the treatment temperature increases, the amount of carbide increases. The calculated proportions of

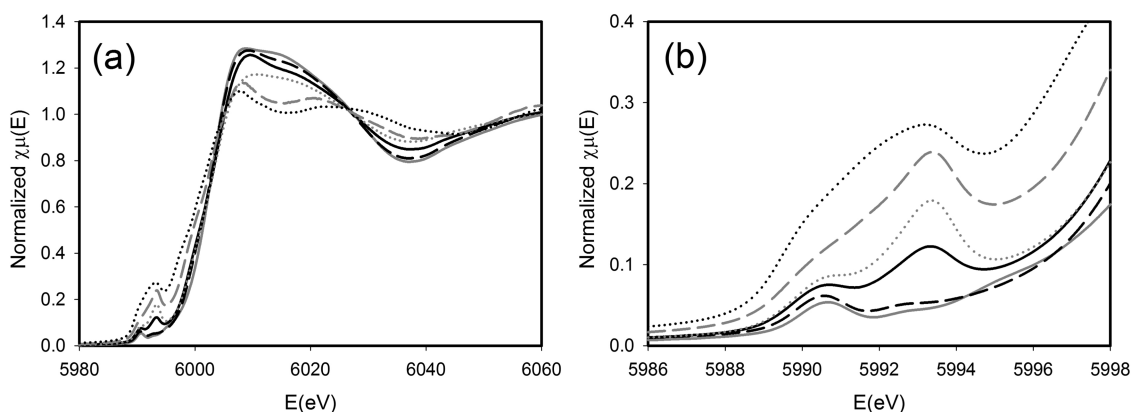


Figure 3. XANES of leather and leather biochar heated to different temperatures. Leather standard (grey solid line); heated in the large vessel at 500 °C (dashed line) or 600 °C (solid line); heated in the small vessel at 600 °C (grey dotted line), 800 °C (grey dashed line), or 1000 °C (dotted line). (a) XANES region. (b) Expanded pre-edge region.

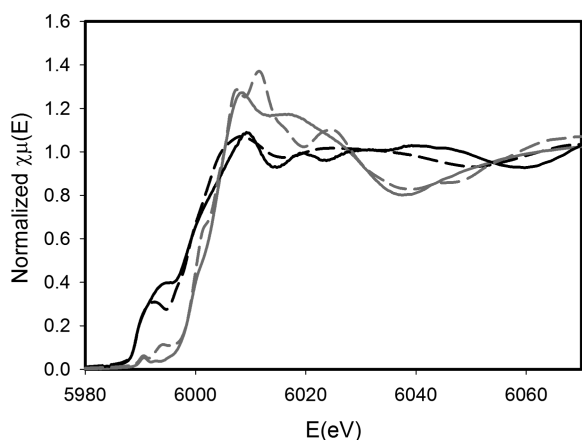


Figure 4. XANES of standards tested for linear combination fit. $\text{Cr}_2(\text{SO}_4)_3$ (grey solid line), Cr_3C_2 (dashed line), Cr metal (solid line), Cr_2O_3 (grey dashed line).

carbide and Cr sulfate (represented as the dry leather spectrum) are listed in Table 2. Fitting to the $k^3\chi(k)$ spectra gives similar proportions of Cr_3C_2 and $\text{Cr}_2(\text{SO}_4)_3 \cdot x\text{H}_2\text{O}$, as does fitting to the energy spectra.

Chromium Carbide Formation. Thermodynamic considerations suggest that, under high carbon activity and low oxygen activity (as in char formation), Cr metal or Cr carbide may form.^{35,36} This occurs at $\log P_{\text{O}_2}$ (bar) below about -16 , with the carbides formed at $\log a_{\text{C}}$ (carbon activity) above about -2.8 (Cr metal forms at lower a_{C}).³⁵ In contrast, during oxy-fuel combustion of coal, Cr(III) in the form of Cr silicate and iron chromite are the dominant species.^{37,38} It is not known exactly what conditions prevail in the char formation in the reaction vessels; however, it is expected that P_{O_2} is low and a_{C} is high, and therefore, it is not surprising that Cr carbide is found in the samples.

Fine atmospheric particulates containing Cr, supposed to be from natural and industrial sources, have been found to contain both Cr^0 and Cr carbide using XANES,³⁹ which demonstrates that Cr carbides are not uncommon in the environment.

It has been reported that carbothermal reduction by pitch of various transition metal oxides, including Cr oxide, forms carbides.⁴⁰ In a N_2 atmosphere or an ammonia atmosphere, nitrides may also be formed for most of the metal oxides studied in that report, with the exception of Cr, which did not

form nitrides, only carbide.⁴⁰ These studies indicate that leather biochar is likely to contain Cr carbide, and not Cr nitride, even if the biochar is formed in the presence of nitrogen. The XANES shows that the Cr changes from the initial, dispersed Cr sulfate to some possibly intermediate compound (which may be a form of carbide) to form a Cr carbide at 1000 °C not dissimilar to Cr_3C_2 .

EXAFS of Biochar for Structural Information. Information about the structural environment of the Cr in the leather biochar is obtained from an analysis of the EXAFS range of the data acquired. Data were processed using VIPER,²⁷ and a Hanning window applied to the Fourier transforms. Theoretical ab initio EXAFS spectra for pairs of atoms were calculated using FEFF6L,⁴¹ with crystal structures from the ATOMS database (Center for Advanced Radiation Sources, University of Chicago). Modeling in k space of the experimental spectra (from selected regions of the Fourier transform) using combinations of EXAFS spectra for these atom pairs was then performed with VIPER.²⁷ To validate the modeling of the EXAFS data, the spectrum of Cr_2O_3 was used, which is a crystalline material with a relatively simpler structure than Cr_3C_2 . The resultant bond lengths are consistent with the crystallographic structure, validating the EXAFS data and fitting and enabling the analysis of the more complex biochar, which XANES has shown to contain a mixture of Cr_3C_2 and other components.

Chromium Carbide. To interpret the EXAFS of the biochar, it is helpful to refer to the literature on EXAFS of Cr carbide. A detailed study of the electronic structure of Cr carbides³¹ notes that crystalline Cr_3C_2 belongs to the space group $pnma$, with lattice parameters $a = 5.485 \text{ \AA}$, $b = 2.789 \text{ \AA}$, and $c = 11.474 \text{ \AA}$. Common phases that may form in Cr-based coatings include Cr_3C_2 , Cr_7C_3 , and Cr_{23}C_6 . Based on the enthalpies of formation, Cr_3C_2 is the most stable of the Cr carbide phases, followed by Cr_7C_3 , with Cr_{23}C_6 and Cr_3C equal third.³¹ The bonding is described as a combination of metallic, ionic and covalent, in character with a strong proportion of metallic character (e.g., metallicity for Cr_3C_2 is estimated at 15% and is higher for the other Cr carbides). The charge on Cr of Cr_3C_2 is calculated to be $\text{Cr}^{+0.33}$.³¹ Bond lengths in these compounds³¹ and in Cr_3C_2 and Cr doped diamond-like carbon (DLC) films obtained from EXAFS⁴² are detailed in Table 3. The bond distances measured in the leather biochar are

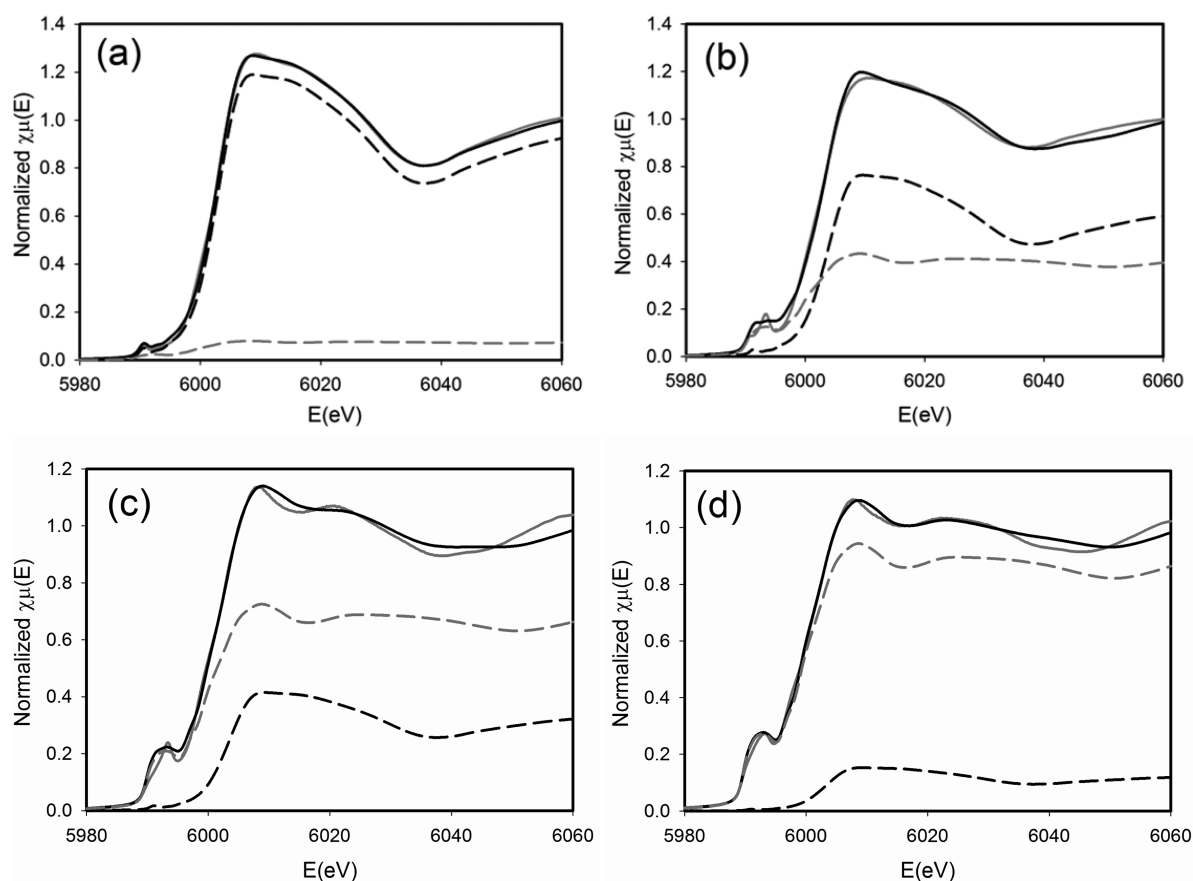


Figure 5. XANES linear combination fit of biochar prepared at (a) 500 °C; (b) 600 °C; (c) 800 °C; and (d) 1000 °C. Cr_3C_2 (grey dashed line), dry leather (dashed line), data (grey solid line), fit (solid line).

Table 2. Chemical Components of Linear Combination Fitting to the XAS Energy Spectrum^a

	$\text{Cr}_2(\text{SO}_4)_3 \cdot x\text{H}_2\text{O}$ (mol % Cr)	Cr_3C_2 (mol % Cr)	R factor ($\times 10^{-4}$), χ^2
biochar 500 °C ^b	93	7	1.7, 0.027
biochar 600 °C ^b	77	23	3.4, 0.051
biochar 600 °C	59	41	5.6, 0.081
biochar 800 °C	35	65	5.8, 0.081
biochar 1000 °C	12	88	2.2, 0.031

^aUncertainty in mole percent Cr in $\text{Cr}_2(\text{SO}_4)_3 \cdot x\text{H}_2\text{O}$ and Cr_3C_2 is around $\pm 5\%$. ^bLarger reaction vessel.

therefore similar to those reported for Cr carbide reported in the literature and to one crystalline compound measured here.

EXAFS of Biochar. There are numerous different atom–atom scattering path lengths in Cr carbide, some of which are quite similar in size. The char formed at 600 °C is too complex a mixture to enable reliable modeling of the EXAFS spectrum. However, the EXAFS spectra of the biochar prepared at 800 and 1000 °C can be fitted with one grouped Cr–C atom pair sets and two grouped Cr–Cr atom pair sets, representing similar atom–atom distances in each group (Figure 6). From the fits, the bond distances shown in Table 4 are obtained. These bond distances are similar to those reported for Cr carbide compounds as listed in Table 3. This EXAFS analysis supports the XANES interpretation and confirms that Cr carbide is formed at higher temperatures.

Stability in the Soil Environment. While it has been found that using acid to produce biochar leachate does not remove Cr from the biochar, long-term stability tests of the material in soil environments were not performed. These would be desirable to ensure the safety of the material for use in agricultural settings. As noted above, oxidation or reduction of

Table 3. Bond Lengths in Cr Carbide Compounds Reported from EXAFS in References 31 and 42

compound	radial distribution peak Cr–C (Å)	radial distribution peak Cr–Cr (Å)	source
Cr_3C	2.12	2.58	31
Cr_3C_2	2.11	2.63	31
Cr_7C_3	2.14	2.58	31
Cr_{23}C_6	2.10	2.56	31
Cr_3C_2	2.2	2.7	42
Cr–DLC	2.17–2.25	2.75–2.79	42

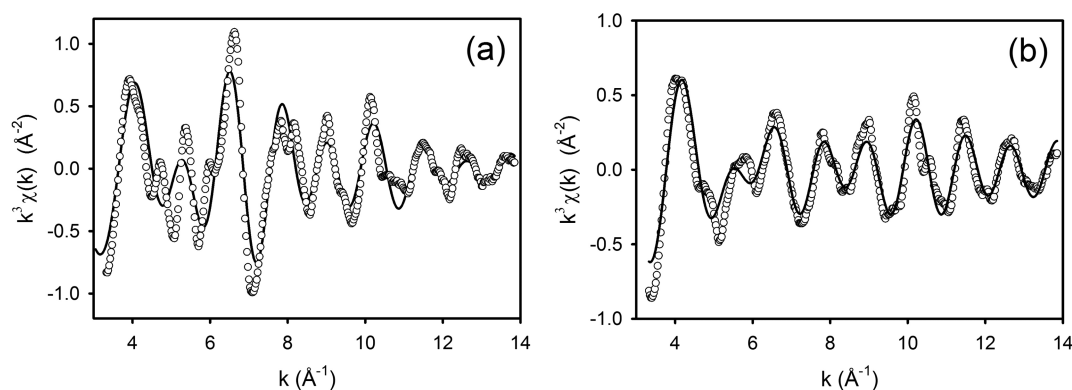


Figure 6. EXAFS of biochar produced at (a) 800 °C and (b) 1000 °C: (circles) $k^3\chi(k)$, (solid line) fitted model.

Table 4. Bond Lengths Obtained from the Modeling of Fourier Transform of EXAFS Spectra of Leather Biochar^a

sample	Cr–C (Å), coordination number	Cr–Cr (Å), coordination number	Cr–Cr (Å), coordination number
biochar 800 °C	2.07, 3.6	2.58, 0.7	2.94, 3.0
biochar 1000 °C	2.05, 1.7	2.70, 4.3	2.92, 1.8

^aSix scattering paths were combined for Cr–C, 12 paths for Cr–Cr in total (in two groups).

some Cr compounds can occur in soils, depending on redox environment of the soil¹⁹ and also such oxidation can be facilitated by bacterial action.⁴³ However, Cr carbide is a very stable material, and is resistant to oxidation or reduction.⁴⁴ The charcoal or biochar matrix within which the Cr is contained is also known to be very stable in soils.⁴⁵ The addition of charcoal to soil enhances the agricultural productivity of the soil, for example in the traditional terra preta soils from South America⁴⁶ but also in more recent studies of soil productivity.¹⁵

CONCLUSIONS

It has been shown that there may be an environmental benefit in making biochar from chrome-tanned leather waste. The char does not release Cr with acid leaching, unlike untreated leather. It has also been shown that the Cr becomes chemically reduced by a carbothermic reaction on charring at high temperatures forming Cr carbide. Cr carbide is an inherently stable compound and its stability is further enhanced by being highly dispersed in a stable carbon medium. Biochar has the added benefits of enhancing agricultural production from soil and providing long-term sequestration of carbon from the environment. This strategy may turn a large-scale waste into an economic resource.

AUTHOR INFORMATION

Corresponding Author

*E-mail: r.haverkamp@massey.ac.nz.

Notes

The authors declare no competing financial interest.

ACKNOWLEDGMENTS

This research was undertaken on the XAS beamline at the Australian Synchrotron, Victoria, Australia. The NZ Synchrotron Group Ltd is acknowledged for travel funding. Clive Bardell and John Edwards, Massey University, built the high-

temperature reactor. The work was supported by Ministry of Business Innovation and Employment grants LSRX0801 and LSRX1202.

REFERENCES

- (1) Commodities and Trade Division, F. A. O., United Nations *World statistical compendium for raw hides and skins, leather and leather footwear 1990–2011*; Rome, 2012.
- (2) Gao, Y.; Xia, J. Chromium contamination accident in china: viewing environment policy of China. *Environ. Sci. Technol.* **2011**, *45* (20), 8605–8606.
- (3) Izbicki, J. A.; Bullen, T. D.; Martin, P.; Schroth, B. Delta Chromium-53/52 isotopic composition of native and contaminated groundwater, Mojave Desert, USA. *Appl. Geochem.* **2012**, *27* (4), 841–853.
- (4) James, B. R. The challenge of remediating chromium-contaminated soil. *Environ. Sci. Technol.* **1996**, *30* (6), A248–A251.
- (5) Heidemann, E. Disposal and recycling of chrome-tanned materials. *J. Am. Leather Chem. As.* **1991**, *86* (9), 331–333.
- (6) Cabeza, L. F.; Taylor, M. M.; DiMaio, G. L.; Brown, E. M.; Mermer, W. N.; Carrio, R.; Celma, P. J.; Cot, J. Processing of leather waste: pilot scale studies on chrome shavings. Isolation of potentially valuable protein products and chromium. *Waste Manage.* **1998**, *18* (3), 211–218.
- (7) Beltran-Prieto, J. C.; Veloz-Rodriguez, R.; Perez-Perez, M. C.; Navarrete-Bolanos, J. L.; Vazquez-Nava, E.; Jimenez-Islas, H.; Botello-Alvarez, J. E. Chromium recovery from solid leather waste by chemical treatment and optimization by response surface methodology. *Chem. Ecol.* **2012**, *28* (1), 89–102.
- (8) Dotro, G.; Castro, S.; Tujchneider, O.; Piovano, N.; Paris, M.; Faggi, A.; Palazolo, P.; Larsen, D.; Fitch, M. Performance of pilot-scale constructed wetlands for secondary treatment of chromium-bearing tannery wastewaters. *J. Hazard. Mater.* **2012**, *239*, 142–151.
- (9) Ashokkumar, M.; Thanikaivelan, P.; Krishnaraj, K.; Chandrasekaran, B. Transforming chromium containing collagen wastes into flexible composite sheets using cellulose derivatives: structural, thermal, and mechanical investigations. *Polym. Composite* **2011**, *32* (6), 1009–1017.
- (10) Przepiorkowska, A.; Chronska, K.; Zaborski, M. Chrome-tanned leather shavings as a filler of butadiene-acrylonitrile rubber. *J. Hazard. Mater.* **2007**, *141* (1), 252–257.
- (11) Erdem, M. Chromium recovery from chrome shaving generated in tanning process. *J. Hazard. Mater.* **2006**, *129* (1–3), 143–146.
- (12) Tahiri, S.; Albizane, A.; Messaoudi, A.; Azzi, M.; Bennazha, J.; Younsi, S. A.; Bouhria, M. Thermal behaviour of chrome shavings and of sludges recovered after digestion of tanned solid wastes with calcium hydroxide. *Waste Manage.* **2007**, *27* (1), 89–95.
- (13) Stam, A. F.; Meij, R.; Winkel, H. T.; van Eijk, R. J.; Huggins, F. E.; Brem, G. Chromium speciation in coal and biomass co-combustion products. *Environ. Sci. Technol.* **2011**, *45* (6), 2450–2456.

- (14) Aitkenhead, W.; Edmonds, R. L. Biochar: A possibility for solid waste disposal. *Leather Int.* **2013**, *215* (4827), 28–30.
- (15) Chan, K. Y.; Van Zwieten, L.; Meszaros, I.; Downie, A.; Joseph, S. Agronomic values of greenwaste biochar as a soil amendment. *Aust. J. Soil Res.* **2007**, *45* (8), 629–634.
- (16) Erdem, M.; Ozverdi, A. Leaching behavior of chromium in chrome shaving generated in tanning process and its stabilization. *J. Hazard. Mater.* **2008**, *156* (1–3), 51–55.
- (17) Oliveira, L. C. A.; Guerreiro, M. C.; Goncalves, M.; Oliveira, D. Q. L.; Costa, L. C. M. Preparation of activated carbon from leather waste: A new material containing small particle of chromium oxide. *Mater. Lett.* **2008**, *62* (21–22), 3710–3712.
- (18) Sekaran, G.; Shanmugasundaram, K. A.; Mariappan, M. Characterization and utilisation of buffing dust generated by the leather industry. *J. Hazard. Mater.* **1998**, *63* (1), 53–68.
- (19) Brose, D. A.; James, B. R. Oxidation-reduction transformations of chromium in aerobic soils and the role of electron-shuttling quinones. *Environ. Sci. Technol.* **2010**, *44* (24), 9438–9444.
- (20) Kappen, P.; Welter, E.; Beck, P. H.; McNamara, J. M.; Moroney, K. A.; Roe, G. M.; Read, A.; Pigram, P. J. Time-resolved XANES speciation studies of chromium on soils during simulated contamination. *Talanta* **2008**, *75* (5), 1284–1292.
- (21) Martin, R. R.; Naftel, S. J.; Sham, T. K.; Hart, B.; Powell, M. A. XANES of chromium in sludges used as soil ameliorants. *Can. J. Chem.* **2003**, *81* (2), 193–196.
- (22) Covington, A. D.; Lampard, G. S.; Menders, O.; Chadwick, A. V.; Rafeletos, G.; O'Brien, P. Extended X-ray absorption fine structure studies of the role of chromium in leather tanning. *Polyhedron* **2001**, *20*, 461–466.
- (23) Reich, T.; Rossberg, A.; Hennig, C.; Reich, G. Characterization of chromium complexes in chrome tannins, leather, and gelatin using extended X-ray absorption fine structure (EXAFS) spectroscopy. *J. Am. Leather Chem. As* **2001**, *96* (4), 133–147.
- (24) ISO. *Leather—Chemical determination of chromic oxide content—Part 1: Quantification by titration*; 2007; Vol. ISO 5398-1:2007 (IULTCS/IUC 8-1).
- (25) ISO. *Leather—Chemical determination of chromic oxide content—Part 3: Quantification by atomic absorption spectrometry*; 2007; Vol. ISO 5398-3:2007 (IULTCS/IUC 8-3).
- (26) Ravel, B.; Newville, M. ATHENA, ARTEMIS, HEPHAESTUS: Data analysis for X-ray absorption spectroscopy using IFEFFIT. *J. Synchrotron Radiat.* **2005**, *12*, 537–541.
- (27) Klementev, K. V. Extraction of the fine structure from x-ray absorption spectra. *J. Phys. D Appl. Phys.* **2001**, *34* (2), 209–217.
- (28) Pantelouris, A.; Modrow, H.; Pantelouris, M.; Hormes, J.; Reinen, D. The influence of coordination geometry and valency on the K-edge absorption near edge spectra of selected chromium compounds. *Chem. Phys.* **2004**, *300* (1–3), 13–22.
- (29) Gardea-Torresday, J. L.; Tiemann, K. J.; Armendariz, V.; Bess-Oberto, L.; Chianelli, R. R.; Rios, J.; Parsons, J. G.; Gamez, G. Characterization of Cr(VI) binding and reduction to Cr(III) by the agricultural byproducts of Avena monida (Oat) biomass. *J. Hazard. Mater.* **2000**, *80* (1–3), 175–188.
- (30) Farges, F. Chromium speciation in oxide-type compounds: application to minerals, gems, aqueous solutions and silicate glasses. *Phys. Chem. Miner.* **2009**, *36* (8), 463–481.
- (31) Li, Y. F.; Gao, Y. M.; Xiao, B.; Min, T.; Yang, Y.; Ma, S. Q.; Yi, D. W. The electronic, mechanical properties and theoretical hardness of chromium carbides by first-principles calculations. *J. Alloy. Compd.* **2011**, *509* (17), 5242–5249.
- (32) de Groot, F.; Vanko, G.; Glatzel, P. The 1s x-ray absorption pre-edge structures in transition metal oxides. *J. Phys.: Condens. Matter* **2009**, *21* (10), DOI: 10.1088/0953-8984/21/10/104207.
- (33) Frommer, J.; Nachtgeal, M.; Czeka, I.; Weng, T. C.; Kretschmar, R. X-ray absorption and emission spectroscopy of Cr-III (hydr)oxides: analysis of the K-pre-edge region. *J. Phys. Chem. A* **2009**, *113* (44), 12171–12178.
- (34) Yamamoto, T. Assignment of pre-edge peaks in K-edge x-ray absorption spectra of 3d transition metal compounds: electric dipole or quadrupole? *X-Ray Spectrom.* **2008**, *37* (6), 572–584.
- (35) Chu, W. F.; Rahmel, A. The conversion of chromium-oxide to chromium carbide. *Oxid. Met.* **1981**, *15* (3–4), 331–337.
- (36) Grabke, H. J.; Krajak, R.; Paz, J. C. N. On the mechanism of catastrophic carburization - metal dusting. *Corros. Sci.* **1993**, *35* (5–8), 1141–1150.
- (37) Jiao, F.; Wijaya, N.; Zhang, L.; Ninomiya, Y.; Hocking, R. Synchrotron-based XANES speciation of chromium in the oxy-fuel fly ash collected from lab-scale drop-tube furnace. *Environ. Sci. Technol.* **2011**, *45* (15), 6640–6646.
- (38) Chen, J.; Jiao, F.; Zhang, L.; Yao, H.; Ninomiya, Y. Use of synchrotron XANES and Cr-doped coal to further confirm the vaporization of organically bound Cr and the formation of chromium-(VI) during coal oxy-fuel combustion. *Environ. Sci. Technol.* **2012**, *46* (6), 3567–3573.
- (39) Werner, M. L.; Nico, P. S.; Marcus, M. A.; Anastasio, C. Use of micro-XANES to speciate chromium in airborne fine particles in the Sacramento Valley. *Environ. Sci. Technol.* **2007**, *41* (14), 4919–4924.
- (40) Eick, B. M.; Youngblood, J. P. Carbothermal reduction of metal-oxide powders by synthetic pitch to carbide and nitride ceramics. *J. Mater. Sci.* **2009**, *44* (5), 1159–1171.
- (41) Rehr, J. J.; Deleon, J. M.; Zabinsky, S. I.; Albers, R. C. Theoretical X-ray absorption fine-structure standards. *J. Am. Chem. Soc.* **1991**, *113* (14), 5135–5140.
- (42) Singh, V.; Palshin, V.; Tittsworth, R. C.; Meletis, E. I. Local structure of composite Cr-containing diamond-like carbon thin films. *Carbon* **2006**, *44* (7), 1280–1286.
- (43) He, J.-Z.; Meng, Y.-T.; Zheng, Y.-M.; Zhang, L.-M. Cr(III) oxidation coupled with Mn(II) bacterial oxidation in the environment. *J. Soils Sediments* **2010**, *10* (4), 767–773.
- (44) Sen, S.; Ozdemir, O.; Demirkiran, A. S.; Sen, U.; Yigit, F.; Hashmi, M. S. J. Oxidation kinetics of chromium carbide coating produced on AISI 1040 steel by thermo-reactive deposition method during high temperature in air. *Adv. Mater. Res.* **2012**, *445*, 649–654.
- (45) Schmidt, M. W. I.; Torn, M. S.; Abiven, S.; Dittmar, T.; Guggenberger, G.; Janssens, I. A.; Kleber, M.; Kogel-Knabner, I.; Lehmann, J.; Manning, D. A. C.; Nannipieri, P.; Rasse, D. P.; Weiner, S.; Trumbore, S. E. Persistence of soil organic matter as an ecosystem property. *Nature* **2011**, *478* (7367), 49–56.
- (46) Glaser, B.; Haumaier, L.; Guggenberger, G.; Zech, W. The 'Terra Preta' phenomenon: a model for sustainable agriculture in the humid tropics. *Naturwissenschaften* **2001**, *88* (1), 37–41.